RSC Advances

PAPER

View Article Online
View Journal | View Issue

Cite this: *RSC Adv.*, 2015, **5**, 56274

Structure and electrochemical performance of hollow microspheres of $LiFe_xNi_{1/3-x}Co_{1/3}Mn_{1/3}O_2$ ($0.000 \leq x \leq 0.267$) as cathodes for lithium-ion batteries

Qing Chang,[a] Heng Zhang,[b] Xujun Wang,[a] Weiquan Shao,[ac] Hongliang Li,[d] Feng Yuan,[ac] Xiangang Xu[b] and Sheng Xu*[ac]

Received 15th May 2015
Accepted 18th June 2015

DOI: 10.1039/c5ra09073c

www.rsc.org/advances

$LiFe_xNi_{1/3-x}Co_{1/3}Mn_{1/3}O_2$ ($0.000 \leq x \leq 0.267$) hollow microspheres have been synthesized by an approach using manganese carbonate microspheres as self-templates and substituting stoichiometric iron for nickel. XRD analysis shows that the obtained materials have a layered α-$NaFeO_2$ structure (rhombohedral lattice, $R\bar{3}m$ space group). With the addition of iron, the lattice parameters of these samples increase in the low-x region ($x \leq 0.133$) and reach their maximum values at $x = 0.133$. The behavior of the lattice parameters is consistent with their specific capacities at 0.1 C rate, which means moderate substitution of iron can enhance the performance. Meanwhile, the iron substitution destroys the hollow microspheres and results in microsphere aggregation, which can be found from their surface morphologies using the SEM analysis. Compared with the others, when x is equal to 0.133, the sample exhibits a relatively superior electrochemical performance.

Introduction

Nowadays, lithium ion batteries (LIBs) are used widely as energy storage systems for a variety of electronic devices such as mobile phones, portable computers, hybrid electric vehicles and so forth.[1,2] LIBs have relatively high stored energy density and a good cycle life, but they cannot satisfy the requirements for electronic products in modern society, which promotes studies on improving the treatments of cathode materials. This is because a better cathode material as the lithium ion source can directly increase the energy density of LIBs.[3,4] Currently, researchers focus on transition metal oxides as LIBs cathode materials and receive many satisfactory results. With a high operating voltage and easy preparation, $LiCoO_2$ becomes the first cathode material of commercial LIBs.[5] However, its high cost due to expensive element Co and toxicity limits its large-scale high power applications.[6] $LiMn_2O_4$ is easily obtained and very cheap, furthermore, it does not pollute the environment, but its disadvantage is bad cycling performance.[7] $LiNiO_2$ is worth concerning with its large capacity and being eco-friendly.[8] Layered $LiNiO_2$ material has a high rate and large power performance, since there are better electronic and Li^+ conductivities in the two-dimensional layer than three-dimensional structure like the spinel $LiMn_2O_4$.[9,10] But it forms NiO_2 during the $LiNiO_2$ phase transition due to lithium ions extraction and insertion, which reduces discharge capacity.[11]

$LiNi_{0.5}Mn_{1.5}O_4$ hollow microspheres/microcubes prepared by a simple impregnation method display a high discharge capacity of 120 mA h g^{-1} and good rate capability until 20 C. When the nickel is substituted for a bit of manganese in $LiMn_2O_4$, the oxidation state of manganese is increased and as a result, the capacity fade resulting from manganese dissolution is controlled effectively.[12] Y. Ding *et al.* have recently reported the double-shelled $LiMn_2O_4$ hollow micro-spheres cathodes prepared by a self-template approach, and this structural $LiMn_2O_4$ has a superior electrochemical performance.[13] It has been explained that the volume of interior space is adjusted automatically to adapt the processes of lithium ion extraction and insertion, which improve significantly the cycle stability. $LiNi_{1/3}Co_{1/3}Mn_{1/3}O_2$ has frequently been investigated by lots of researchers because of its stable structure, large discharge capacity and low cost, but unfortunately bad rate capacity and fast capacity fade always prevent its practical applications.[14–16] Using the porous spinel $Mn_{1.5}Co_{1.5}O_4$ hollow microspheres as template, J. Li *et al.* have synthesized $LiNi_{1/3}Co_{1/3}Mn_{1/3}O_2$ hollow microspheres, which exhibit excellent electrochemical performances.[17] P. Mohan *et al.* have synthesized $LiFe_xNi_{1-x}O_2$ ($0.00 \leq x \leq 0.20$) nanoparticles by sol–gel approach and this material has single layer structure. Through the substitution of

[a]College of Physics, Qingdao University, Qingdao 266071, China. E-mail: shengxu@qdu.edu.cn; Tel: +86-532-85953968
[b]State Key Laboratory of Crystal Material (Shandong University), Jinan 250100, China
[c]Key Laboratory of Photonics Materials & Technology in Universities Shandong (Qingdao University), Qingdao 266071, China
[d]College of Chemical, Science and Engineering, Qingdao University, Qingdao 266071, China

iron, particles size are reduced and so electrochemical properties of these cathodes are improved, especially as x is equal to 0.15.[18] In order to study structure and electrochemical performance of doped $LiNi_{1/3}Co_{1/3}Mn_{1/3}O_2$ hollow microspheres, we do this research.

In this work, we investigate the hollow microspheres of $LiFe_xNi_{1/3-x}Co_{1/3}Mn_{1/3}O_2$ ($0.000 \leq x \leq 0.267$), which are synthesized by substituting stoichiometric iron for nickel in $LiNi_{1/3}Co_{1/3}Mn_{1/3}O_2$ obtained through $MnCO_3$ microspheres as self-template. According to XRD, SEM analysis and electrochemical testing, it is shown that there is a corresponding relation between structures and specific capacities of the synthesized cathode materials. Meanwhile, it reveals that moderate iron addition can improve the electrochemical performance, but it would destroy the hollow microspherical structure if too much iron was doped. There are some good properties particularly when x is equal to 0.133.

Experimental

Materials synthesis

The $MnCO_3$ microspheres about 5 μm were prepared by a simple precipitation method reported in the literature.[19] Firstly, 1.183 g of $MnSO_4$ and 5.53 g of NH_4HCO_3 were separately dissolved in 500 mL of ultrapure water with a conductivity of 0.05 μS cm^{-1}. Then 50 mL of ethanol was poured into the $MnSO_4$ solution. After the mixed solution was completely dispersion and turned transparent, the NH_4HCO_3 solution was added to it at room temperature with vigorous stirring. After a while, the mixture became increasingly white, which represented there were some $MnCO_3$ precipitations to form. The above suspension was maintained for 5 h. Then the upper solution of obtained mixture was removed and $MnCO_3$ microspheres can be separated from the lower solution by centrifugation. Finally, the mixture of ultrapure water and ethanol was used to wash $MnCO_3$ precipitations and they were dried in a vacuum oven (60 °C, 0.1 MPa) for 6 h.

$MnCO_3$ microspheres were decomposed at 400 °C for 9 h to obtain MnO_2 microspheres. Stoichiometric amounts of MnO_2 microspheres, $LiOH \cdot H_2O$, $Ni(NO_3)_2 \cdot 6H_2O$, $Fe(NO_3)_3 \cdot 9H_2O$ and $Co(NO_3)_2 \cdot 6H_2O$ [metal ions ratio Li : Fe : Ni : Co : Mn = $1 : x : (1/3 - x) : 1/3 : 1/3$] ($x$ = 0–0.267) were dissolved in the ethanol with continuous stirring until all ethanol evaporated. Final products were obtained by thermal treatment at 850 °C for 12 h.

Characterization

The X-ray diffraction (XRD) patterns were collected on a D8 Advance instrument with Cu Kα radiation, $2\theta = 10$–$70°$ with the step of 0.02°, and the exposure time was for 20 min. The JEOL JSM-6390 scanning electron microscope (SEM) was used to analyze the morphologies of the obtained products.

Electrochemical measurements

The electrochemical measurements were performed using CR2025 coin cells on a LAND CT2001A battery tester at room temperature. The working electrodes were prepared by pasting slurries of the active materials ($LiFe_xNi_{1/3-x}Co_{1/3}Mn_{1/3}O_2$), carbon black, and poly(vinylidene fluoride) (PVDF) binder at a weight ratio of 8 : 1 : 1 in N-methyl-2-pyrrolidone (NMP) onto aluminum foil and followed by drying overnight at 120 °C in a vacuum. The coin cells were assembled in a glove box (H_2O < 1 ppm, O_2 < 1 ppm) using lithium metal foil as the anode and 1 M $LiPF_6$ in a 1 : 1 v/v mixture of ethylene carbonate and diethyl carbonate as the electrolyte. The charge–discharge cycles were carried out at different rates with the voltage range of 2.5–4.5 V. Electrochemical impedance spectra (EIS) were measured over the frequency range of 0.1 Hz to 100 kHz on an electro-chemical workstation PARSTAT 2273. Cyclic voltammetry (CV) was tested at a scan rate of 0.1 mV s^{-1} and in the potential range of 2.5–4.5 V.

Results and discussion

The surface morphologies of the $LiFe_xNi_{1/3-x}Co_{1/3}Mn_{1/3}O_2$ ($0.000 \leq x \leq 0.267$) samples are clearly illustrated in Fig. 1. The hollow microspheres are about 5 μm in the diameter from Fig. 1a and f. However, with the iron substitution, hollow microspheres are gradually destroyed and microspheres begin to aggregate in Fig. 1b–e, which decreases specific surface area and lithium ion diffusion, and directly results in the specific capacities reducing and resistances enhancing.

The XRD patterns of obtained $LiFe_xNi_{1/3-x}Co_{1/3}Mn_{1/3}O_2$ ($0.000 \leq x \leq 0.267$) powder materials are analyzed with the RIETAN-FP program.[20] With Rietveld analysis performed, the structural paraments of these powder materials have been attained in Table 1, and the final refinements are reliable as the values of

$$R_{wp}\left(\equiv\left[\frac{\sum_i w_i\left(y_i - y_{i,\mathrm{calc}}\right)^2}{\sum_i w_i {y_i}^2}\right]^{1/2}\right),\quad R_I\left(\equiv\frac{\sum_k \left|I_{k,\mathrm{calc}} - I_k\right|}{\sum_k \left|I_{k,\mathrm{calc}}\right|}\right)$$

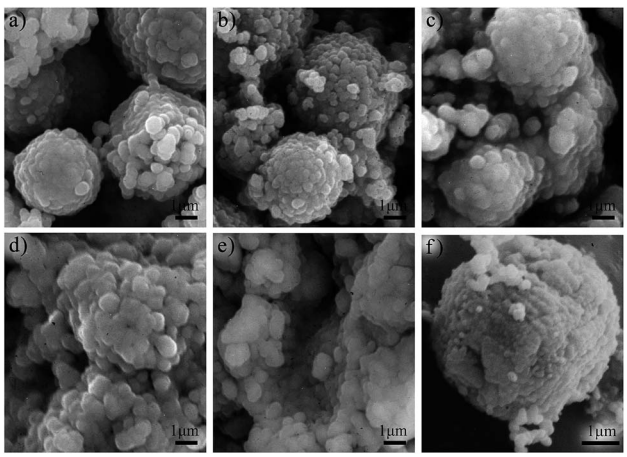

Fig. 1 SEM images of (a)–(e) $LiFe_xNi_{1/3-x}Co_{1/3}Mn_{1/3}O_2$ ($0.000 \leq x \leq 0.267$) samples and (f) a broken hollow microsphere.

Table 1 $LiFe_xNi_{1/3-x}Co_{1/3}Mn_{1/3}O_2$ ($0.000 \leq x \leq 0.267$) structural paraments refined by the RIETAN-FP

x	a (Å)	c (Å)	V (Å^3)	R_{wp} (%)	R_I (%)	S
0.000	2.84(8)	14.20(3)	99.8(0)	3.291	5.041	1.1199
0.067	2.85(2)	14.21(7)	100.1(8)	3.142	3.048	1.0716
0.133	2.85(8)	14.26(9)	100.9(5)	3.216	3.032	1.0219
0.200	2.85(3)	14.25(9)	100.4(9)	3.188	1.974	1.0539
0.267	2.84(4)	14.21(5)	99.5(7)	3.116	4.243	1.0650

and S ($\equiv R_{wp}/R_e$, in which R_e is statistically minimal value of R_{wp}) are small enough. All the samples have layered α-$NaFeO_2$ structure (rhombohedral lattice with the $R\bar{3}m$ space group), and their structural paraments are slightly different. Refined XRD patterns of all samples are similar, so the prototypical example of XRD powder pattern of $LiFe_xNi_{1/3-x}Co_{1/3}Mn_{1/3}O_2$ ($x = 0.133$) is exhibited in Fig. 2, where the red crosses are measured points, green sticks peak positions, solid green line fitted curve and blue line error curve. Meanwhile, most of reflections are clearly indexed in the parenthesis.

The Fig. 3a indicates that with the addition of iron, lattice parameters a and c of these samples increase in the low-x region ($x \leq 0.133$) and reach their maximum values at $x = 0.133$. Lattice parameters a and c of these samples increase with further increase of x. These behavior is similar to the change of their discharge specific capacities at 0.1 C rate in Fig. 3b. It is concluded that the iron has entered $LiFe_xNi_{1/3-x}Co_{1/3}Mn_{1/3}O_2$ crystal lattice, and moderate substitution of iron can enhance specific capacity of the sample. That is because the increased lattice parameters provide lithium ion insertion/extraction process with a favourable condition. As $x = 0.133$, discharge capacity (205.4 mA h g^{-1}) is larger than the others and the morphology after charge and discharge cycles sustains initial structure, hence we investigate more about $x = 0.133$ below.

Electrochemical performance of the $LiFe_xNi_{1/3-x}Co_{1/3}Mn_{1/3}O_2$ ($x = 0.133$) cathode was investigated between 2.5 and 4.5 V at different rates with the anodes of lithium metal. The charge/discharge curves are illustrated in Fig. 4a for various cycles at the rate of 0.1 C. From these smooth curves, it shows that the electrode material has a stable structure within the

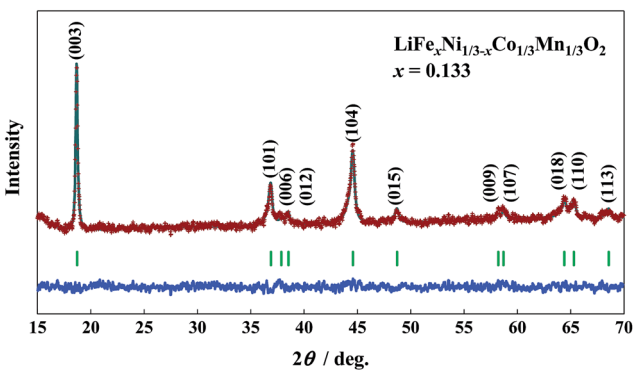

Fig. 2 XRD pattern of the $LiFe_xNi_{1/3-x}Co_{1/3}Mn_{1/3}O_2$ ($x = 0.133$) powder material.

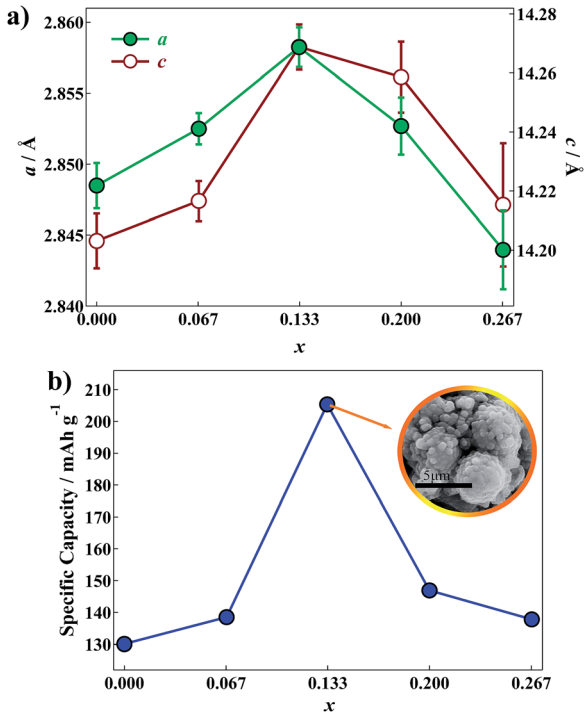

Fig. 3 (a) Lattice parameters and (b) specific capacities in the fifth cycle at 0.1 C rate of the $LiFe_xNi_{1/3-x}Co_{1/3}Mn_{1/3}O_2$ ($0.000 \leq x \leq 0.267$) samples. Inset is morphology of $x = 0.133$ after cycles.

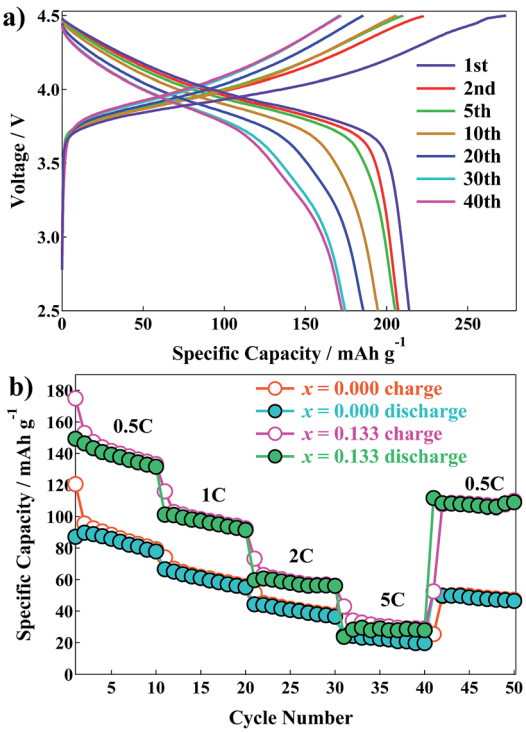

Fig. 4 (a) Charge/discharge curves of $LiFe_xNi_{1/3-x}Co_{1/3}Mn_{1/3}O_2$ ($x = 0.133$) cathode at the rate of 0.1 C. (b) Rate capabilities of the $LiFe_xNi_{1/3-x}Co_{1/3}Mn_{1/3}O_2$ ($x = 0$, 0.133) cathodes.

voltage range.[21] The first charge capacity of this sample is 273.6 mA h g^{-1}, and the discharge capacity 213.9 mA h g^{-1}. Through the first cycle, it exhibits the irreversible capacity is lost, perhaps because the film of solid electrolyte interphase (SEI) is formed in this process.

Fig. 4b shows rate capabilities of the $LiFe_xNi_{1/3-x}Co_{1/3}Mn_{1/3}O_2$ ($x = 0, 0.133$) cathodes in voltage range between 2.5 and 4.5 V at various rates. It demonstrates that doped specific capacities are larger than the pure one in every rate, and gradually decreasing with the rates increasing. Moreover, the capacities can almost go back to the initial values while the rate returns to 0.1 C. From this, one can infer that the cathode material has an excellent reversibility. The good rate capabilities are due to the doped iron ions not only increasing the lattice parameters, but also advancing the lithium ions extraction and insertion. In addition, the hollow microspherical structure enlarges the contact surface between electrolyte and electrode.

Cyclic voltammograms of the $LiFe_xNi_{1/3-x}Co_{1/3}Mn_{1/3}O_2$ ($x = 0, 0.133$) electrodes were measured at the scan rate of 0.1 mV s^{-1} with voltage range of 2.5–4.5 V, and shown in Fig. 5a. Lithium ions were inserted and extracted from $LiFe_xNi_{1/3-x}Co_{1/3}Mn_{1/3}O_2$ during the cathodic and anodic sweep. Meanwhile, there is a reduction peak and an oxidation peak formed at 3.53 V and 3.8 V separately in cathode ($x = 0.133$). The potential difference between the cathodic and anodic peaks shows the reversibility of the lithium ions intercalation and deintercalation, and the larger this value is, the more strongly electrode polarizes. It can be found that 0.27 V, the potential interval of the doped cathode is smaller than 0.28 V of the pure one, which indicates the sample at $x = 0.133$ has a lower electrode polarization and a better reversibility than the pure one.

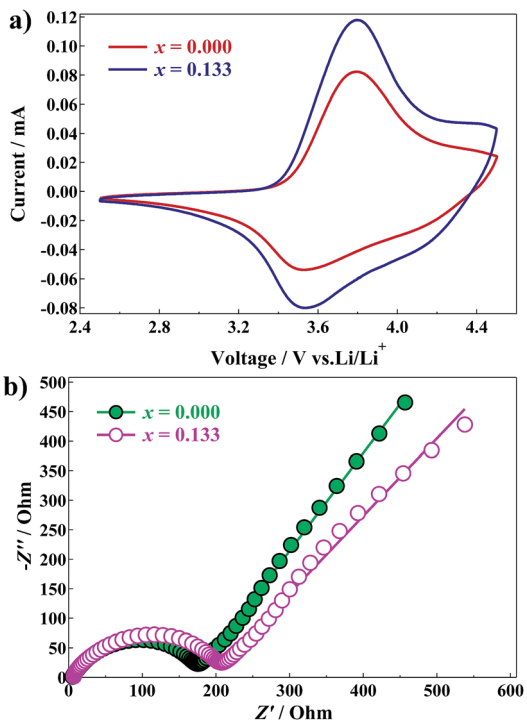

Fig. 5 (a) Cyclic voltammetry curves of the $LiFe_xNi_{1/3-x}Co_{1/3}Mn_{1/3}O_2$ ($x = 0, 0.133$) cathodes. (b) Electrochemical impedance spectra of the $LiFe_xNi_{1/3-x}Co_{1/3}Mn_{1/3}O_2$ ($x = 0, 0.133$) cathodes.

In order to study the influence of doping for electrochemical impedance, we measure the EIS of $LiFe_xNi_{1/3-x}Co_{1/3}Mn_{1/3}O_2$ ($x = 0, 0.133$) using three electrode cells over the frequency range from 0.1 Hz to 100 kHz, and the results are illustrated in the Fig. 5b. In this plot, there are an oblique line and a combined semicircle. The Z'-intercept in high frequency is the ohmic resistance (R_e) resulting from the resistances of cell components and electrolyte. The middle frequency semicircle is associated with the charge transfer resistance (R_{ct}), which occurs at the interface of the electrode with electrolyte. The oblique line of low frequency is Warburg impedance (Z_w) related to the lithium ions diffusion in the cathode materials.[22] One may found that the charge transfer resistance is 205.3 Ω at $x = 0.133$, which is larger than 175.6 Ω with no doped one. It represents that the hollow microspherical structure is destroyed and it occurs microspheres aggregation with the addition of iron, hence the charge transfer resistance is increased. The larger value is also corresponding to the result of the surface morphology from SEM analysis.

Conclusions

In summary, taking manganese carbonate microspheres as self-template and substituting iron were used to fabricate the $LiFe_xNi_{1/3-x}Co_{1/3}Mn_{1/3}O_2$ ($0.000 \leq x \leq 0.267$) hollow microspheres as cathodes for LIBs. Lattice parameters with specific capacities increase in the low-x region ($x \leq 0.133$) and decrease in the high-x region ($x \geq 0.133$) with the addition of iron, which indicates moderate iron can improve performance for LIBs. Whereas, although hollow microspherical structure enhances performance, the iron substitution increases microspheres aggregation, and also reduces electrochemical properties as decreasing lithium ion diffusion. In particular, the material as $x = 0.133$, displays a large capacity, good rate capability and superior reversibility.

Notes and references

1 M. Armand and J.-M. Tarascon, *Nature*, 2008, **451**, 652.
2 H.-K. Song, K. T. Lee, M. G. Kim, L. F. Nazar and J. Cho, *Adv. Funct. Mater.*, 2010, **20**, 3818.
3 M. M. Thackeray, C. Wolverton and E. D. Isaacs, *Energy Environ. Sci.*, 2012, **5**, 7854.
4 A. S. Arico, P. Bruce, B. Scrosati, J. M. Tarascon and W. V. Schalkwijk, *Nat. Mater.*, 2005, **4**, 366.
5 B. L. Ellis, K. T. Lee and L. F. Nazar, *Chem. Mater.*, 2010, **22**, 691.
6 K. Ozawa, *Solid State Ionics*, 1994, **69**, 212.
7 D. S. Ahn and M. Y. Song, *J. Electrochem. Soc.*, 2000, **147**(3), 874.
8 J. R. Dahn, U. V. Sacken, M. W. Juzkow and H. A. Janaby, *J. Electrochem. Soc.*, 1991, **138**, 2207.
9 J. Kim, B. H. Kim, Y. H. Baik, P. K. Chang, H. S. Park and K. Amine, *J. Power Sources*, 2006, **158**, 641.
10 J. M. Tarascon, E. Wang, F. K. Shokoohi, W. R. Mekinnon and S. Colsons, *J. Electrochem. Soc.*, 1991, **38**, 2859.

11 T. Ohzuku, A. Ueda and M. Nagayama, *J. Electrochem. Soc.*, 1993, **140**, 1563.
12 L. Zhou, D. Y. Zhao and X. W. Lou, *Angew. Chem., Int. Ed.*, 2012, **51**, 239.
13 Y.-L. Ding, X.-B. Zhao, J. Xie, G.-S. Cao, T.-J. Zhu, H.-M. Yu and C.-Y. Sun, *J. Mater. Chem.*, 2011, **21**, 9475.
14 N. Yabuuchi, Y. Makimura and T. Ohzuku, *J. Electrochem. Soc.*, 2007, **154**, A314.
15 J. Dou, X. Kang, T. Wumaier, H. Yu, N. Hua, Y. Han and G. Xu, *J. Solid State Electrochem.*, 2012, **16**, 1481.
16 J. Li, C. Cao, X. Xu, Y. Zhu and R. Yao, *J. Mater. Chem. A*, 2013, **1**, 11848.
17 J. Li, S. Xiong, Y. Liu, Z. Ju and Y. Qian, *Nano Energy*, 2013, **2**, 1249.
18 P. Mohan and G. P. Kalaignan, *J. Electroceram.*, 2013, **31**, 210.
19 J. Fei, Y. Cui, X. Yan, W. Qi, Y. Yang, K. Wang, Q. He and J. Li, *Adv. Mater.*, 2008, **20**, 452.
20 F. Izumi and K. Momma, *Solid State Phenom.*, 2007, **130**, 15.
21 C. Nithya, V. S. Syamala Kumari and S. Gopukumar, *Phys. Chem. Chem. Phys.*, 2011, **13**, 6125.
22 X. Huang, H. Chen, S. Zhou, Y. Chen, J. Yang, Y. Ren, H. Wang, M. Qu, Z. Pan and Z. Yu, *Electrochim. Acta*, 2012, **60**, 239.

